



Carrier transport mechanism in aluminum nanoparticle embedded AlQ_3 structures for organic bistable memory devices

V.S. Reddy, S. Karak, S.K. Ray, A. Dhar*

Department of Physics and Meteorology, IIT Kharagpur, Kharagpur 721 302, India

ARTICLE INFO

Article history:

Received 4 July 2008

Received in revised form 2 October 2008

Accepted 16 October 2008

Available online 31 October 2008

PACS:

72.80.Le

73.61.Ph

85.30.De

85.65.+h

Keywords:

Organic semiconductor

Memory device

Conduction mechanism

Nanoparticle

ABSTRACT

Electrical bistability is demonstrated in organic memory devices based on *tris*-(8-hydroxyquinoline)aluminum (AlQ_3) and aluminum nanoparticles. The role of the thickness of middle aluminum layer and the size of the nanoparticles in device performance is investigated. Above a threshold voltage, the device suddenly switches from a low conductivity OFF state to a high conductivity ON state with a conductivity difference of several orders of magnitude. The OFF state of the device could be recovered by applying a relatively high voltage pulse. The electronic transition is attributed to an electric field induced transfer of charge between aluminum nanoparticles and AlQ_3 . The type of charge carriers responsible for conductance switching is investigated. The charge carrier conduction mechanism through the device in ON and OFF states is studied by temperature dependent current–voltage characteristics and analyzed in the framework of existing theoretical models. The conduction mechanism in the OFF state is dominated by field-enhanced thermal excitation of charge carriers from localized centers, whereas it changes to Fowler–Nordheim tunneling of charge carriers in the ON state. The device exhibited excellent stability in either conductivity states. The results indicate the strong potential of the device towards its application as a nonvolatile electronic memory.

© 2008 Elsevier B.V. All rights reserved.

1. Introduction

During the past fifteen years, tremendous work has been done in the field of organic semiconductor based electronic devices. Devices such as light emitting diodes [1–3], field effect transistors [4–6] and solar cells [7–9] have shown great potential towards future technologies. Organic semiconductor based devices exhibit unique advantages such as low fabrication cost, high mechanical flexibility and versatility of the material chemical structure compared with the inorganic semiconductor devices. However, to widen the application of organic semiconductors to varieties of electronics systems, organic based memory devices are essential [10–16]. The basic feature of a memory device is to exhibit bistable behavior having two different resistance states at the same applied voltage. Ma et al. have

demonstrated memory effects in a three layer organic/metal nanoparticle/organic structure embedded between two electrodes [17]. Bozano and coworkers have studied the important role of different metal nanoparticles in a three layer memory structure [18]. During the device operation, when applied voltage exceeds a certain value, the device suddenly switches from a low conductivity ‘OFF’ state to a high conductivity ‘ON’ state, with a conductivity difference of several orders of magnitude. This high conductivity state will be memorized until an ‘OFF’ voltage is applied to erase it. Despite the superior performance of organic memory devices, the charge carrier transport mechanism in the ‘ON’ and ‘OFF’ states and the type of carriers responsible for bistability are not understood clearly.

In this paper, we describe the fabrication and operation of the tri-layer organic/metal/organic and the single layer memory structures sandwiched between two electrodes. The effect of the thickness of intermediate metal layer and the size of the nanoparticles in device performance is

* Corresponding author. Tel.: +91 3222 283830; fax: +91 3222 255303.
E-mail address: adhar@phy.iitkgp.ernet.in (A. Dhar).

investigated. The charge carrier conduction mechanism through the device in 'ON' and 'OFF' states is studied by temperature dependent current–voltage characteristics and analyzed in terms of existing theoretical models. The type of carriers responsible for conductance switching is also investigated.

2. Experimental

In present investigation, three different types of device structures were studied. The first type (type-I) is the tri-layer AlQ_3/Al nanoislands/ AlQ_3 structure sandwiched between two electrodes (hereafter called tri-layer device), the second one (type-II) is a single AlQ_3 layer embedded between two electrodes (hereafter called single layer device), and the third type (type-III) is the ITO/Poly(3,4-ethylenedioxythiophene)-poly(styrenesulfonate) (PEDOT:PSS)/ AlQ_3/Al nanoislands/ AlQ_3/Al device. For all types of devices, patterned indium tin oxide (ITO) (SPI Inc.) with sheet resistance $10 \Omega/\square$ was used as the bottom electrode. Prior to AlQ_3 deposition, ITO substrates were cleaned thoroughly in acetone, isopropyl alcohol and de-ionized water in sequence by an ultrasonic cleaner followed by drying with nitrogen gas. For the fabrication of tri-layer structure, both the AlQ_3 and Al middle layers were deposited by thermal evaporation at a base pressure of 5×10^{-6} mbar. The thickness of the each AlQ_3 layer was about 50 nm and that of the middle Al layer was varied between 5 and 20 nm. The deposition rate of the middle Al layer was controlled by a quartz crystal thickness monitor. In order to obtain the nanoscale metal islands, a low evaporation rate of less than 0.1 nm/s was used. For the single layer device structure, AlQ_3 (100 nm) was thermally evaporated on ITO electrodes. For the fabrication of ITO/PEDOT:PSS/ AlQ_3/Al nanoislands/ AlQ_3/Al device, a 40 nm thick PEDOT:PSS layer was spin coated on ITO substrates from a 2.8 wt.% water solution (Aldrich). Post baking was done for 1 h at around 110 °C to remove the solvent completely. Deposition of all other layers of this device was done in the same manner as the tri-layer device. Finally, aluminum top electrode strips were deposited by thermal evaporation through a shadow mask.

The thickness of different layers was monitored by quartz crystal monitor and was verified by stylus profilometer (Veeco Dektak3). Cross sectional scanning electron

microscopy (SEM) images of the device were taken using a ZEISS SUPRA 40 field emission (FE) microscope. Atomic force microscopy (AFM) (Veeco Nanoscope-IV) in tapping mode was used to evaluate the surface morphology of the middle Al layer. Fourier-transform infrared (FTIR) spectra of the middle Al layer in the wave number range $400\text{--}4000 \text{ cm}^{-1}$ were obtained using a Nexus 870 Thermo Nicolet spectrometer. The optical transmission spectra were measured in the wavelength range 300–1100 nm using a UV–vis–NIR spectrophotometer (Perkin–Elmer Lambda 45). The dc current–voltage characteristics of the devices were obtained using a Keithley 485 Pico ammeter and an Advantest R6144 programmable dc voltage generator.

3. Results and discussion

Fig. 1 shows the cross sectional view of a typical tri-layer memory structure (type-I) sandwiched between ITO and Al electrodes. The FE–SEM micrograph clearly indicates ITO, two AlQ_3 layers and Al layer with sharp interfaces. The thickness of bottom AlQ_3 , top AlQ_3 , ITO and Al layers are estimated to be 70 nm, 50 nm, 400 nm and 200 nm, respectively.

The performance of organic bistable device is sensitive to metal nanoparticles and the thickness of the middle metal layer. The ON/OFF current ratio, for example, depends strongly on the size and density of the nanoparticles. Morphology and the thickness of the middle Al layer depends on the evaporation rate and is controlled by quartz crystal monitor. Films deposited with a higher deposition rate led to continuous films and, hence, non-switching devices. A deposition rate less than 0.1 nm/s resulted in island like growth and bistable devices. Detailed information about the nanostructure of the middle Al layer has been obtained by AFM. Fig. 2a illustrates the surface morphology of the middle Al layer of thickness 5 nm. It clearly shows disconnected metal islands of various sizes. The size distribution of nanoislands is estimated from this AFM image and is shown in Fig. 2b. The island size varies from 5 nm to about 25 nm with peak of the distribution at 15 nm. When the thickness of the film is increased to 10 nm, the size of nanoislands increases slightly as shown in Fig. 2c. For this film the island size distribution ranges from 8 nm to about 35 nm and peaks at 20 nm, as shown in Fig. 2d. The gaps

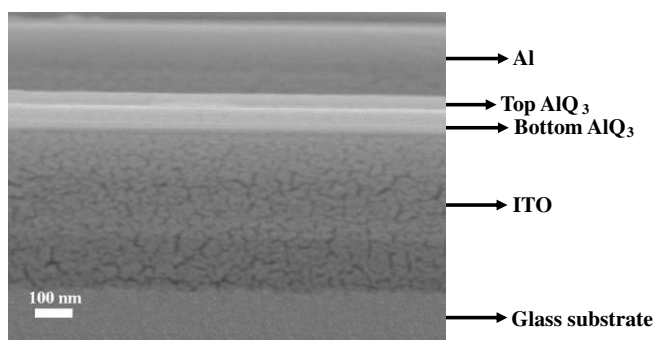


Fig. 1. Cross sectional SEM image of the tri-layer memory device, ITO/ $\text{AlQ}_3/\text{Al}/\text{AlQ}_3/\text{Al}$ (type-I).

Download English Version:

<https://daneshyari.com/en/article/1268278>

Download Persian Version:

<https://daneshyari.com/article/1268278>

[Daneshyari.com](https://daneshyari.com)